Synthesis and Characterization of Copper Oxide-Titanium Dioxide One-Dimensional Composites for Photocatalysis

Aseel Adnan Ouda[1] and Firas Kamil Mohamad[2]
[1]*Ministry of Education, Educational Directorate of Holy Kerbala, 56001 Kerbala, Iraq*
[2]*Department of Physics, College of Science, University of Kerbala, 56001 Kerbala, Iraq*
aseeladnanalobaidi@gmail.com, firas.k.m@uokerbala.edu

Keywords: Micro-Rise-Like Structure, Composite, Polyol Method, CuO/TiO_2.

Abstract: In the present paper, efficient and low-cost metal oxide systems, such as one-dimensional (1D) CuO/TiO_2 submicro-composites, were synthesized via a two-step polyol-mediated solvothermal process. Titanium(IV) isopropoxide and copper(II) nitrate trihydrate were used as precursors. The CuO/TiO_2 composites were prepared by varying the CuO loading (1 and 3 wt.%) and calcined at 450 °C for three hours. The effect of CuO doping on the structural and morphological properties of TiO_2 was investigated using X-ray diffraction (XRD), field-emission scanning electron microscopy (FESEM), and energy-dispersive X-ray spectroscopy (EDX). The structural findings for all the prepared samples showed anatase with a tetragonal crystal structure. The morphological image confirmed that the TiO_2 and CuO dopant nanoparticles bound together, forming a nano-rise-like structure. The results showed that the length of the CuO/TiO_2 composite decreased with increasing weight percentage. The CuO/TiO_2 composite at 1 wt.% exhibited the optimal average length and diameter of 2.902 μm and 0.406 μm, respectively, compared to the 3 wt.% composite. According to these findings, the obtained TiO_2-doped CuO can be used as a binary metal oxide for visible-light photocatalytic applications.

1 INTRODUCTION

Numerous semiconducting metal oxides have been employed in photocatalytic processes. Among several oxide metal nanoparticles, titanium dioxide (TiO_2) is considered the preferred photocatalyst due to its unique properties, including high stability, affordability, non-toxicity, and abundance on Earth [1]. In addition to its electronic band positions, the conduction and valence bands align with the redox potential of water. The redox potential, or oxidation-reduction potential, refers to the tendency of matter to either gain or lose electrons in a chemical reaction, indicating its ability to act as an oxidizing or reducing agent [2]. However, TiO_2 has a significant limitation in that, a wide band gap (approximately 3.2 eV), which limits its light absorption mainly to ultraviolet (UV) light. Therefore, TiO_2 absorption is limited to the ultraviolet region, which accounts for only 3-5% of the solar spectrum [3]. To overcome this, TiO_2 is often modified through compositing or doping with other materials to enhance its visible-light absorption. Using one-dimensional nanostructures in the composite process is expected to enhance efficiency compared to their bulk or nanoparticle counterparts, due to their extraordinary surface-to-volume relationship [4]. TiO_2 nanostructures, such as rods, wires, belts, and tubes, have demonstrated improved photocatalytic efficiency due to quantum confinement effects on charge carriers [5]. Moreover, the fundamental problem with the pure TiO_2 nanostructure photocatalyst is due to low surface area, which is affected by poor visible-spectrum absorption and low crystallinity [6]. The surface area of TiO_2 nanoparticles significantly impacts their photocatalytic efficiency. Several studies have shown that a higher surface area increases reactivity and light interaction, enhancing photocatalytic performance [7]-[9]. To convert TiO_2 nanostructures into effective photocatalysts, researchers have employed the doping methods, such as noble-metal doping [10]-[13]. Noble metals doped into TiO_2 nanoparticles have been shown to be highly effective in increasing their photocatalytic efficiency [14]-[16]. However, the noble metal dopants, including gold (Au), platinum (Pt), silver (Ag), and palladium (Pd), are highly costly and not rare-earth abundant.

Therefore, it became necessary to identify alternative, low-cost, and highly effective nanomaterials. The preparation of composites by combining TiO_2 nanoparticles with other semiconductor materials with small energy gaps has broadened the materials' absorption to a broader region of the solar spectrum [17]. One of the best semiconductor metal oxides, copper oxide (CuO), appears to be a promising candidate because of its small band gap (1.4-1.9 eV), non-toxic, non-noble, and cheaper nature. Furthermore, CuO and TiO_2 can form a p-n heterojunction, which is highly effective for charge-carrier separation [18]-[20]. As a result, photoexcited electrons are injected from the band of conduction (CB) of TiO_2 to the band of conduction of CuO. In contrast, holes are built up in the valence band, which has a higher positive potential [21]. Several methods have been reported for synthesizing CuO/TiO_2 composites; for instance, Lu et al. prepared a CuO/TiO_2 composite via the hydrolysis method [22]. Asrai et. al. prepared a CuO/TiO_2 nanocomposite via solvothermal processing [23]. Yaqi Li synthesized CuO/TiO_2 nanocomposite using a simple deposition technique [24]. CuO/TiO_2 nanocomposites were successfully prepared using the hydrothermal method by Zhuang et. al. [25]. Mingmongkol et al. synthesized TiO_2 doped with CuO nanoparticles using the sol-gel method at various concentrations [26]. Yu et. al. prepared CuO/TiO_2 nanocomposites in a rod-like structure via a microwave-assisted method [27]. In the present study, the polyol-mediated solvothermal method is a relatively straightforward approach for preparing the CuO/TiO_2 composites with longer 1D structures and excellent crystallinity.

2 EXPERIMENTAL PART

2.1 Chemicals and Materials

All chemical materials were utilized as received without any additional purification. Titanium (IV) isopropoxide (TTIP, 98% Acros Organics) $C_{12}H_{28}O_4Ti$, was used as a TiO_2 precursor. Ethylene glycol (EG, J.T. Baker 99.8% Anhydrous solvent) $C_2H_4(OH)_2$ was used as a solvent to control the condensation rate of TTIP. Cupric (II) nitrate trihydrate (95%, J.T. Baker, Inorganic salt) $Cu(NO_3)_2.3H_2O$ as a doping agent precursor. Absolute ethanol (99.5% J.T. Baker Reagent), C_2H_5OH, and deionized water (DIW, highly pure) were utilized to remove any residual organic species for the preparation process of the product. Ammonium hydroxide solution (99.9%, J.T. Baker, basic), NH_4OH, was used for pH adjustments. All the raw materials were purchased from the local market in Baghdad, Iraq.

2.2 Preparation of CuO/TiO_2 Composite

A 1D TiO_2 Submicro-Rise-like structure was prepared by a facile two-step polyol-mediated solvothermal method. In the first step, 100 mL of EG was put in a 250 mL glass reaction vessel and heated to 170 °C using a hot plate with magnetic stirring. Then, 2.5 mL of TTIP was gradually added to the EG solution. After the mixing process, white titanium glycolate precipitates were obtained. The mixing procedure continued for 5 hours at a constant stirring rate of 800 rpm. After the mixing period, the solution was left to cool down to 75 °C. In the second step, different concentrations of copper nitrate trihydrate were dissolved in 10 mL of absolute ethanol in a vessel, and the mixture was stirred for 10 min. This sub-reaction formed the blue solution. Then, the copper precursor solution was added dropwise to the white titanium glycolate precipitates, which were stirred at a rising temperature to 170 °C again. The copper precursor was already condensed on the TiO_2 nanosurface by adding drops of NH_4OH under constant stirring until the pH reached 6. The resultant light-blue suspension solution was stirred for an additional hour. Finally, the light-blue nanopowders were collected by centrifugation. Then, the obtained powders were repeatedly washed with absolute ethanol and ultrapure water to remove any residual organic impurities. The CuO/TiO_2 nanopowders were obtained by drying in an oven at 80 °C in air for 6 hours, followed by calcination at 450 °C for 3 hours.

2.3 Characterization

The crystal structure and crystalline phases of the as-prepared samples were obtained using an X-ray diffractometer (XRD, Aeris, Panalytical, Holland) with monochromatic Cu Kα radiation operated at 40 kV and 15-40 mA, and λ = 1.5418 Å. The prepared specimens were scanned over the 2θ range 5-90° with a step size of 0.05°/s to obtain the XRD patterns. The Scherrer formula was applied to estimate the crystalline specimen size based on the XRD pattern.

$$D = k \lambda / \beta \cos\theta, \quad (1)$$

where D is the crystallite size in nm, k is the shape factor (equal to 0.9 for spherical crystallites), λ is the wavelength of X-ray radiation in Å (λ=1.5418 Å), β

is the full width at half maximum for the measured peak, and θ is Bragg's angle in radians [28]. The sample morphology was examined using a field-emission scanning electron microscope (FESEM; FEI, Inspect F50, USA). The instrument was coupled with an EDX detector to scan the selected samples, producing a map of components and identifying the chemical elements.

3 RESULTS AND DISCUSSION

3.1 Structural Results

Figure 1 shows the X-ray diffraction patterns of undoped TiO_2 and (1 and 3 wt.%) CuO/TiO_2 composite samples prepared via a two-step polyol-mediated solvothermal process and calcined at a temperature of 450 °C for 3h. The XRD diffraction pattern of undoped TiO_2 Submicro 1D matched well with the standard data of anatase TiO_2 powders, which were referenced from the Joint Committee on Powder Diffraction Standards (JCPDS), No. 021-1272. This fact refers to the formation of TiO_2 nanopowders as shown in Figure 1a. No XRD diffraction peaks of other titanium polymorphs indicate that the TiO_2 has a high-purity phase. XRD of the doped concentrations 1 wt.%, and 3 wt.% CuO/TiO_2 composites showed diffraction patterns like the undoped TiO_2, with the additional sharper peaks due to CuO particle doping into the TiO_2 rise-like structure, as shown in Figure 1b and c. Due to the CuO homogeneous dispersion at these loading concentrations, they lacked an adequate dimension to generate a distinctive XRD pattern. However, the presence of CuO particles in TiO_2 nanostructures affects the surface area, band gap, particle size, and quantum output of the resulting catalysts. From the diffraction pattern, it was found that the TiO_2 crystalline planes were observed at (101), (004), (200), (105), (204), (220), (215), (224), which occurred at 2θ = 25.3°, 37.8°, 48.0°, 55.1°, 62.7°, 70.3, 75.1°, and 82.7° respectively. The values of the angle diffraction (2θ) at which the peaks occur correspond to the as-prepared CuO/TiO_2 specific crystal planes. The position peak deviation was not observed because the Cu^{2+} dopant ions occupied the Ti^{4+} substitutional sites, preventing lattice distortion [29]. Moreover, the Cu^{2+} ionic radius of about 0.73 Å was similar to that of the Ti^{4+} ion, 0.74 Å, which allowed the dopant Cu^{2+} ion to replace Ti^{4+} on the TiO_2 structure [30]. The crystal size of the CuO/TiO_2 composite samples was calculated by the Scherrer formula at the (1 1 0) plane. The sharp peak observed at this plane corresponded to a diffraction angle of 2θ = 25.3°, indicating that the prepared materials had a well-tetragonal crystalline structure. The crystal size of CuO/TiO_2 composite samples appeared generally smaller than that of undoped TiO_2 nanoparticles. When the CuO dopant was increased, the samples' crystallite size reduced from 7.10 nm for CuO/TiO_2 1 wt.% to 6.50 nm for CuO/TiO_2 3 wt.%. CuO doping successfully reduced the TiO_2 crystalline size by inhibiting crystallisation of the prepared TiO_2 nanoparticles. The XRD findings were summarized in Table 1.

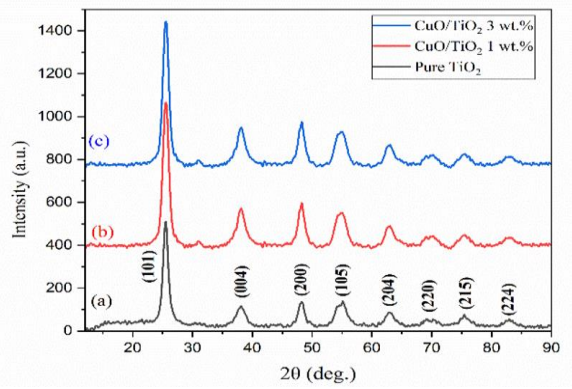

Figure 1: XRD patterns of (a) TiO_2, (b) 1 wt.%, and (c) 3 wt.%, CuO/TiO_2 composites prepared by the polyol-mediated solvothermal method.

Table 1: The crystal size of undoped TiO_2 and doped with CuO particles.

Sample	Average crystallite size (D) nm
TiO_2	7.50
CuO/TiO_2 1wt.%	7.10
CuO/TiO_2 3wt.%	6.50

3.2 Morphological Results

The morphology of undoped TiO_2 and CuO/TiO_2 samples prepared at different weight percentages showed that all synthesized samples exhibit a 1D Submicro-Rise-Like structure, characterized by a cylindrical shape that fills from the inside. No significant difference is observed in the image morphologies of anatase-phase TiO_2 doped with various concentrations of CuO particles, as shown in Figure 2(a-c). The images showed that CuO particles were successfully incorporated into the 1D TiO_2 crystalline. Employing a high-viscosity solvent, such as ethylene glycol (EG), was the most important factor in forming rise-like structures. EG solvent was confirmed to have less nanoparticle aggregation and promote the regular growth of 1D structures. From the FESEM analysis, it was observed that the

obtained CuO/TiO_2 composite samples varied in length, but were shorter than the undoped TiO_2 nanostructures. The average lengths and diameters of the as-prepared pure TiO_2 were found to be about 3.171 µm and 0.417 µm, respectively, as noted in Figure 2(a). The average lengths and diameters of the obtained undoped TiO_2 and CuO/TiO_2 composites were summarized in Table 2. The FESEM image also showed a good distribution of CuO dopant on the surface of the TiO_2 at different doping weight percentages. The CuO particles appeared on all TiO_2 nanostructure samples. Even though the CuO loading concentration was a low amount, Cu^{2+} ions were still discovered on the prepared surface of TiO_2. On the other hand, when the CuO doping concentration increased to 3 wt.%, the obtained photocatalyst began to have a shorter length than the other prepared samples, as observed in Figures 2(b) and (c). The average lengths of the CuO/TiO_2 composites at 1 and 3 wt.% were about 2.902 µm and 2.448 µm, respectively. Whilst the average diameters were about 0.406 µm and 0.385 µm, respectively. The shorter obtained samples result from the slightly larger ion size of $Cu^{2+,}$ which induces internal strain in the TiO_2 nanostructure and causes local lattice distortion [31].

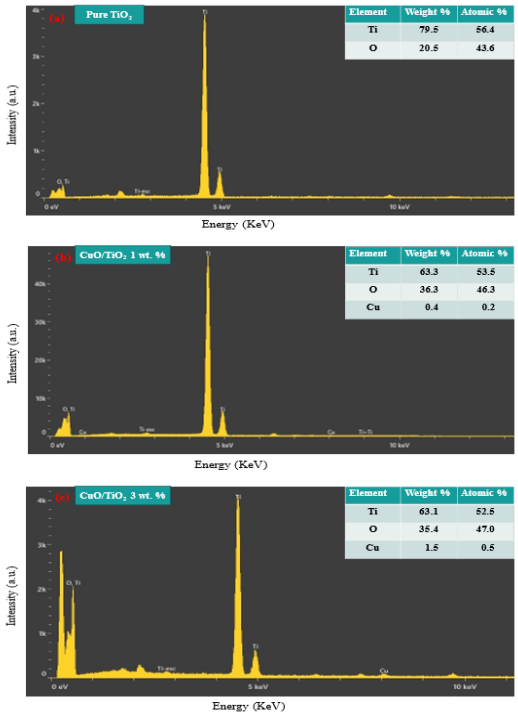

Figure 2: FESEM micrographs of (a) bare TiO_2 powders, (b) 1 wt.%, and (c) 3 wt.% CuO/TiO_2 composite samples.

Table 2: The average lengths and diameters of pure $TiO_2$and CuO/TiO_2 composite samples.

Sample	Average length (µm)	Average diameter (µm)
TiO_2	3.171	0.417
CuO/TiO_2 1 wt.%	2.902	0.406
CuO/TiO_2 3 wt.%	2.448	0.385

3.3 Energy Dispersion Results

Energy-dispersive X-ray beam spectroscopy (EDX) was used to perform quantitative chemical compositional analysis of undoped TiO_2 and CuO/TiO_2 composite samples at different concentrations. The EDX spectrum affirmed the presence of three essential elements: titanium (Ti), oxygen (O), and copper (Cu) in both prepared samples, as shown in Figure 3(a, b, and c). From the EDX analyses, it was noted that Cu nanoparticle was successfully introduced into the TiO_2 structures. The weight and atomic percentage of the elemental composition in CuO/TiO_2 composites were summarized in Figure 3.

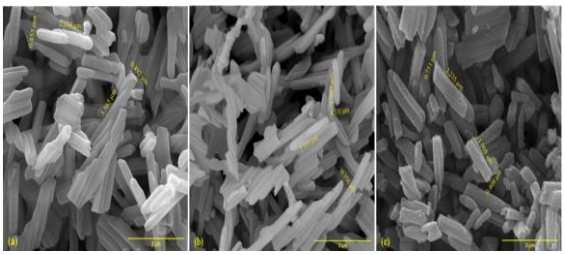

Figure 3: EDX spectrum of (a) TiO_2, 1 wt.% CuO/TiO_2, and 3 wt.% composite samples.

4 CONCLUSIONS

TiO_2 powders and CuO/TiO_2 metal oxide structures were successfully prepared at 170 °C using a two-step polyol-mediated solvothermal method. Titanium isopropoxide and copper nitrate trihydrate were used as raw materials. In this study, ethylene glycol (EG) was used as a synthetic solvent, which governs the photocatalyst quantum yield, crystalline phase, obtained size, and surface morphology. Moreover, due to its high viscosity, EG controls particle aggregation in the preparation process. The XRD, FESEM, and EDX results indicated that CuO and TiO_2 nanoparticles were bound together, forming the CuO/TiO_2 composite. Different concentrations of CuO dopant in the TiO_2, such as 1 wt.% and 3 wt.%, were used. The average length of the prepared

CuO/TiO_2 composite decreased with increasing weight percentage of CuO loading. The most significant length of the binary metal oxide composite was presented by 1 wt.% CuO-doped TiO_2, which was found to have approximately 2.902 μm. These findings confirmed that the polyol method was a facile, low-cost, and favourable route for preparing binary metal oxide CuO/TiO_2 in one-dimensional nanostructures, which can be applied to the preparation of various mixed metal oxides as heterojunctions of interest. Therefore, the cooperative interaction between two metal oxides can be investigated in the catalytic application of an organic dye in wastewater.

ACKNOWLEDGMENTS

The authors are grateful to the College of Science at the University of Kerbala, particularly the Physics Department, for their support and provision of the necessary laboratory equipment.

REFERENCES

[1] S. Bbumba, C. Arum, M. Kigozi, I. Karume, H. Nsamba, I. Kiganda, M. Murungi, J. Ssekatawa, R. Nazziwa, and C. Yikii, "Modified titanium dioxide nanoparticles for photocatalytic splitting of water and its application in environmental remediation as a potential alternative," Asian Journal of Chemical Sciences, vol. 14, pp. 60–73, 2024.

[2] Z. Guo, F. Ambrosio, W. Chen, P. Gono, and A. Pasquarello, "Alignment of redox levels at semiconductor–water interfaces," Chemistry of Materials, vol. 30, pp. 94–111, 2018.

[3] S. Khan, M. Zapata, D. Baptista, R. Gonçalves, J. Fernandes, J. Dupont, M. Santos, and S. Teixeira, "Effect of oxygen content on the photoelectrochemical activity of crystallographically preferred oriented porous Ta_3N_5 nanotubes," The Journal of Physical Chemistry C, vol. 119, pp. 19906–19914, 2015.

[4] A. Machín, K. Fontánez, J. Arango, D. Ortiz, J. León, S. Pinilla, V. Nicolosi, F. Petrescu, C. Morant, and F. Márquez, "One-dimensional (1D) nanostructured materials for energy applications," Materials, vol. 14, p. 2609, 2021.

[5] Z. Zhao, J. Tian, Y. Sang, A. Cabot, and H. Liu, "Structure, synthesis, and applications of TiO_2 nanobelts," Advanced Materials, vol. 27, pp. 2557–2582, 2015.

[6] W. Buraso, V. Lachom, P. Siriya, and P. Laokul, "Synthesis of TiO_2 nanoparticles via a simple precipitation method and photocatalytic performance," Materials Research Express, vol. 5, p. 115003, 2018.

[7] H. Zhou, X. Sheng, J. Xiao, Z. Ding, D. Wang, X. Zhang, J. Liu, R. Wu, X. Feng, and L. Jiang, "Increasing the efficiency of photocatalytic reactions via surface microenvironment engineering," Journal of the American Chemical Society, vol. 142, pp. 2738–2743, 2020.

[8] S. Ullah, E. Neto, A. Khan, I. Medeiros, and H. Wender, "Supported nanostructured photocatalysts: the role of support–photocatalyst interactions," Photochemical and Photobiological Sciences, vol. 22, pp. 219–240, 2023.

[9] Z. Hosseini, F. Haghparast, A. Masoudi, and A. Mortezaali, "Enhanced visible photocatalytic performance of undoped TiO_2 nanoparticle thin films through modifying the substrate surface roughness," Materials Chemistry and Physics, vol. 279, p. 125530, 2022.

[10] F. Irfan, M. Tanveer, M. Moiz, S. Husain, and M. Ramzan, "TiO_2 as an effective photocatalyst: mechanisms, applications, and dopants: a review," The European Physical Journal B, vol. 95, p. 184, 2022.

[11] T. Natarajan, V. Mozhiarasi, and R. Tayade, "Nitrogen-doped titanium dioxide (N–TiO_2): synopsis of synthesis methodologies, doping mechanisms, property evaluation and visible light photocatalytic applications," Photochem, vol. 1, pp. 371–410, 2021.

[12] A. Kumar, P. Choudhary, A. Kumar, P. Camargo, and V. Krishnan, "Recent advances in plasmonic photocatalysis based on TiO_2 and noble metal nanoparticles for energy conversion, environmental remediation, and organic synthesis," Small, vol. 18, p. 2101638, 2022.

[13] J. Jeon, D. Kweon, B. Jang, M. Ju, and J. Baek, "Enhancing the photocatalytic activity of TiO_2 catalysts," Advanced Sustainable Systems, vol. 4, p. 2000197, 2020.

[14] T. Ravishankar, M. Vaz, T. Ramakrishnappa, S. Teixeira, J. Dupont, R. Pai, and G. Banuprakash, "The heterojunction effect of Pd on TiO_2 for visible light photocatalytic hydrogen generation via water splitting reaction and photodecolorization of trypan blue dye," Journal of Materials Science: Materials in Electronics, vol. 29, pp. 11132–11143, 2018.

[15] N. Ibrahim, W. Leaw, D. Mohamad, S. Alias, and H. Nur, "A critical review of metal-doped TiO_2 and its structure–physical properties–photocatalytic activity relationship in hydrogen production," International Journal of Hydrogen Energy, vol. 45, pp. 28553–28565, 2020.

[16] P. Ribao, J. Corredor, M. Rivero, and I. Ortiz, "Role of reactive oxygen species on the activity of noble metal-doped TiO_2 photocatalysts," Journal of Hazardous Materials, vol. 372, pp. 45–51, 2019.

[17] T. Ravishankar, M. Vaz, S. Khan, T. Ramakrishnappa, S. Teixeira, G. Balakrishna, G. Nagaraju, and J. Dupont, "Enhanced photocatalytic hydrogen production from Y_2O_3/TiO_2 nanocomposites: a comparative study on hydrothermal synthesis with and without an ionic liquid," New Journal of Chemistry, vol. 40, pp. 3578–3587, 2016.

[18] D. Yu, L. Xu, H. Zhang, J. Li, W. Wang, L. Yang, X. Jiang, and B. Zhao, "A new semiconductor-based SERS substrate with enhanced charge collection and improved carrier separation: CuO/TiO_2 pn heterojunction," Chinese Chemical Letters, vol. 34, p. 107771, 2023.

[19] L. Gnanasekaran, R. Pachaiappan, P. Kumar, T. Hoang, S. Rajendran, D. Durgalakshmi, M. Moscoso, L. Cornejo-Ponce, and F. Gracia, "Visible light driven exotic p-(CuO)–n-(TiO_2) heterojunction for the photodegradation of 4-chlorophenol and antibacterial activity," Environmental Pollution, vol. 287, p. 117304, 2021.

[20] J. Brito, F. Tavella, C. Genovese, C. Ampelli, M. Zanoni, G. Centi, and S. Perathoner, "Role of CuO in the modification of the photocatalytic water splitting behavior of TiO_2 nanotube thin films," Applied Catalysis B: Environmental, vol. 224, pp. 136–145, 2018.

[21] P. Hajipour, A. Eslami, A. Bahrami, A. Abari, F. Saber, R. Mohammadi, and M. Mehr, "Surface modification of TiO_2 nanoparticles with CuO for visible-light antibacterial applications and photocatalytic degradation of antibiotics," Ceramics International, vol. 47, pp. 33875–33885, 2021.

[22] D. Lu, O. Zelekew, A. Abay, Q. Huang, X. Chen, and Y. Zheng, "Synthesis and photocatalytic activities of a CuO/TiO_2 composite catalyst using aquatic plants with accumulated copper as a template," RSC Advances, vol. 9, pp. 2018–2025, 2019.

[23] A. A'srai, M. Razali, K. Amin, and U. Osman, "CuO/TiO_2 nanocomposite photocatalyst for efficient MO degradation," Digest Journal of Nanomaterials and Biostructures, vol. 18, 2023.

[24] Y. Li, "Electrochemical photocatalytic degradation of brilliant blue FCF as food dye by CuO–TiO_2 nanocomposite under visible and UV-light irradiations," International Journal of Electrochemical Science, vol. 16, p. 210928, 2021.

[25] Q. Zhuang, K. Shi, J. Wang, H. Zhou, P. Zhao, and Y. Lou, "Revolutionizing pollution control with innovative CuO@TiO_2 nanocomposite for enhanced photocatalytic degradation and antimicrobial efficacy," Surfaces and Interfaces, vol. 55, p. 105410, 2024.

[26] Y. Mingmongkol, D. Trinh, D. Channei, W. Khanitchaidecha, and A. Nakaruk, "Decomposition of dye pigment via photocatalysis process using CuO–TiO_2 nanocomposite," Materials Today: Proceedings, vol. 47, pp. 3441–3444, 2021.

[27] Y. Yu, Y. Chen, and Z. Cheng, "Microwave-assisted synthesis of rod-like CuO/TiO_2 for high-efficiency photocatalytic hydrogen evolution," International Journal of Hydrogen Energy, vol. 40, pp. 15994–16000, 2015.

[28] M. Rabiei, A. Palevicius, A. Monshi, S. Nasiri, A. Vilkauskas, and G. Janusas, "Comparing methods for calculating nanocrystal size of natural hydroxyapatite using X-ray diffraction," Nanomaterials, vol. 10, p. 1627, 2020.

[29] T. Raguram and K. Rajni, "Synthesis and analysis of structural, optical, morphological, photocatalytic and magnetic properties of TiO_2 and doped (Ni and Cu) TiO_2 nanoparticles by sol–gel technique," Applied Physics A, vol. 125, pp. 1–11, 2019.

[30] L. Isa, "Synthesis and characterization of structural nanocomposite titanium dioxide copper-doped using the impregnation method," Spektra: Jurnal Fisika dan Aplikasinya, vol. 5, pp. 21–30, 2020.

[31] K. Prajapat, U. Mahajan, M. Dhonde, K. Sahu, and P. Shirage, "Synthesis and characterization of TiO_2 nanoparticles: unraveling the influence of copper doping on structural, surface morphology, and optical properties," Chemical Physics Impact, vol. 8, p. 100607, 2024.